

# Cycloheptatrienyl–Cyclopentadienyl–Zirconium Sandwich Complexes: Structure and Bonding<sup>†</sup>

Matthias Tamm,<sup>\*,‡</sup> Andreas Kunst,<sup>‡</sup> Thomas Bannenberg,<sup>‡</sup>  
Eberhardt Herdtweck,<sup>‡</sup> and Rochus Schmid<sup>§</sup>

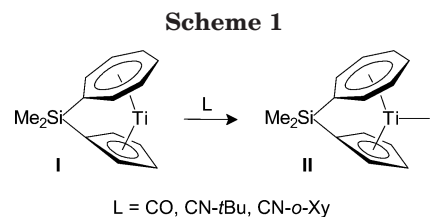
*Lehrstuhl für Anorganische Chemie, Department Chemie, Technische Universität München, Lichtenbergstrasse 4, D-85747 Garching, Germany, and Lehrstuhl für Anorganische Chemie II, Organometallics and Materials Chemistry, Ruhr-Universität Bochum, D-44780 Bochum, Germany*

Received March 15, 2005

The reactions of the 16-electron cycloheptatrienyl–cyclopentadienyl–zirconium sandwich complex  $[(\eta^7\text{-C}_7\text{H}_7)\text{Zr}(\eta^5\text{-C}_5\text{H}_5)]$  (**1**) with *tert*-butyl isocyanide (*t*BuNC) and 2,6-dimethylphenyl isocyanide (*o*-XyNC) have been studied. The isocyanide complexes  $[(\eta^7\text{-C}_7\text{H}_7)(\eta^5\text{-C}_5\text{H}_5)\text{Zr}(\text{CNR})]$  (R = *t*Bu, **2a**; R = *o*-Xy, **2b**) can be isolated in quantitative yield as stable orange (**2a**) or red (**2b**) crystalline solids. The CN stretching vibrations are observed at 2156 (**2a**) and 2134  $\text{cm}^{-1}$  (**2b**) in KBr, indicating a relatively weak zirconium–isocyanide interaction. Solution NMR studies consequently reveal that the isocyanides quickly exchange on the NMR time scale at room temperature. The equilibrium reaction of **1** with *t*BuNC has been examined in further detail by dynamic NMR spectroscopy, allowing an enthalpy for the formation of **2a** of  $\Delta H^\circ = -39.6 \pm 6.6 \text{ kJ mol}^{-1}$  to be established. DFT calculations reveal that the weakness of the zirconium–isocyanide bonds in **2a** and **2b** can be attributed to the strong and appreciably covalent zirconium–cycloheptatrienyl interaction, leading to highly stabilized frontier orbitals and consequently to a diminishing  $\pi$ -electron release capability and a small propensity to efficiently interact with  $\sigma$ -donor/ $\pi$ -acceptor ligands. The X-ray crystal structures of **1** and **2a** are also reported.

## 1. Introduction

Since the serendipitous synthesis and discovery of ferrocene,<sup>1</sup> a plethora of transition-metal sandwich complexes containing predominantly  $\eta^5$ -cyclopentadienyl (Cp) as well as  $\eta^6$ -arene ligands have been studied experimentally and theoretically in great detail.<sup>2</sup> In contrast, comparatively little use has been made of cycloheptatrienyl (Cht) ligands, although mixed cycloheptatrienyl–cyclopentadienyl complexes of the type  $[(\eta^7\text{-C}_7\text{H}_7)\text{M}(\eta^5\text{-C}_5\text{H}_5)]$  (M = group 4–6 metal) have been known for more than three decades.<sup>3</sup> Only recently have the first sandwich complexes containing a silicon bridge between the Cht and Cp rings been reported, which could be obtained by the reaction of  $[(\eta^7\text{-C}_7\text{H}_7)\text{Ti}(\eta^5\text{-C}_5\text{H}_5)]$  (troticene) or  $[(\eta^7\text{-C}_7\text{H}_7)\text{V}(\eta^5\text{-C}_5\text{H}_5)]$  (trovacene) with 2 equiv of *n*-BuLi/*N,N,N',N'*-tetramethylethylenediamine (tmeda) followed by treatment of the intermediate dilithio complexes with  $\text{Me}_2\text{SiCl}_2$ .<sup>4,5</sup> The resulting



*ansa*-Cht–Cp complexes are highly strained molecules, which have been shown to be susceptible to strain release by undergoing ring-opening polymerization reactions.<sup>6</sup> In addition, it could be demonstrated that the bending of the two rings in the 16-electron [1]silatroticeneophane **I** creates a gap at the titanium center, which thereby becomes accessible to monodentate ligands such as CO or isocyanides. Since the resulting complexes **II** give rise to strong diagnostic IR absorptions, the reactivity of **I** toward these  $\sigma$ -donor/ $\pi$ -acceptor ligands could be used to probe its electronic structure, thus revealing that **I** does not behave like a complex containing titanium in a lower oxidation state but, rather, bears a closer resemblance to Lewis acidic  $\text{Ti}^{\text{IV}}$  complexes (Scheme 1). On the basis of theoretical calculations, this behavior can be mainly attributed to a strong and appreciably covalent titanium–cycloheptatrienyl inter-

\* To whom correspondence should be addressed. Tel: +49-89-289/13080. Fax: +49-89-289/13473. E-mail: matthias.tamm@ch.tum.de.

<sup>†</sup> Dedicated to Prof. Dr. Wolf-Walther du Mont (Braunschweig) on the occasion of his 60th birthday.

<sup>‡</sup> Technische Universität München.

<sup>§</sup> Ruhr-Universität Bochum.

(1) Special Issue: 50th Anniversary of the Discovery of Ferrocene. Adams, R. D., Ed. *J. Organomet. Chem.* **2001**, 637–639, 1.

(2) (a) *Comprehensive Organometallic Chemistry*; Wilkinson, G., Stone, F. G. A., Abel, E. W., Eds.; Pergamon Press: Oxford, U.K., 1982.

(b) *Comprehensive Organometallic Chemistry II*; Abel, E. W., Stone, F. G. A., Wilkinson, G., Eds.; Chapman and Hall: Oxford, U.K., 1995.

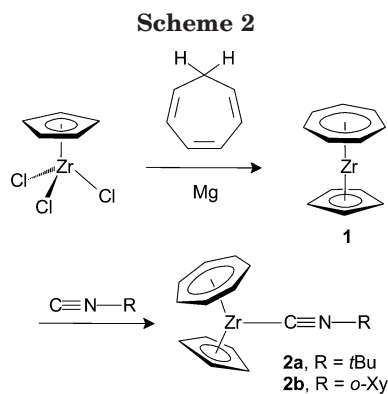
(c) *Metallocenes*; Togni, A., Halterman, R. L., Eds.; Wiley-VCH: Weinheim, Germany, 1998.

(3) Green, M. L. H.; Ng, D. K. P. *Chem. Rev.* **1995**, 95, 439.

(4) Tamm, M.; Kunst, A.; Bannenberg, T.; Herdtweck, E.; Sirsch, P.; Elsevier, C. J.; Ernsting, J. M. *Angew. Chem.* **2004**, 116, 5646; *Angew. Chem., Int. Ed.* **2004**, 43, 5530.

(5) Elschenbroich, C.; Paganelli, F.; Nowotny, M.; Neumüller, B.; Burghaus, O. Z. *Anorg. Allg. Chem.* **2004**, 630, 1599.

(6) Tamm, M.; Kunst, A.; Herdtweck, E. *Chem. Commun.* **2005**, 1729.



action, leading to a highly stabilized frontier orbital and consequently to a diminishing  $\pi$ -electron release capability.<sup>4</sup>

Whereas coordination of additional ligands to the titanium atom has never been observed for unbridged troiticene,  $[(\eta^7\text{-C}_7\text{H}_7)\text{Ti}(\eta^5\text{-C}_5\text{H}_5)]$ , the formation of thermally labile phosphine adducts has been reported for related zirconium and hafnium indenyl complexes of the type  $[(\eta^7\text{-C}_7\text{H}_7)\text{M}(\eta^5\text{-C}_9\text{H}_7)]$ . Only for M = Hf could a dinuclear complex containing a bridging 1,2-bis(dimethylphosphino)ethane (dmpe) ligand be structurally characterized.<sup>7</sup> These findings suggest that the interaction of Cht–Cp–zirconium and –hafnium complexes with  $\sigma$ -donor/ $\pi$ -acceptor ligands such as CO and isocyanides should be possible without the prerequisite of introducing a bridging unit and to synthesize highly strained *ansa*-complexes. Accordingly, we wish to give a detailed experimental and theoretical account of the reactivity of  $[(\eta^7\text{-C}_7\text{H}_7)\text{Zr}(\eta^5\text{-C}_5\text{H}_5)]$  (**1**) toward alkyl and aryl isocyanides in order to assess the strength of the zirconium–isocyanide interaction as well as to probe the electronic structure of the cycloheptatrienyl sandwich complex **1**.

## 2. Results and Discussion

**Synthesis and Characterization of Cycloheptatrienyl–Zirconium Sandwich Complexes.** The cycloheptatrienyl–cyclopentadienyl sandwich complexes  $[(\eta^7\text{-C}_7\text{H}_7)\text{Zr}(\eta^5\text{-C}_5\text{R}_5)]$  (R = H, CH<sub>3</sub>) have been prepared by treating a mixture of the corresponding trichlorides  $[(\eta^5\text{-C}_5\text{R}_5)\text{ZrCl}_3]$  and cycloheptatriene, C<sub>7</sub>H<sub>8</sub>, with a reducing agent such as *i*PrMgCl or magnesium.<sup>8,9</sup> In our hands,  $[(\eta^7\text{-C}_7\text{H}_7)\text{Zr}(\eta^5\text{-C}_5\text{H}_5)]$  (**1**) could be isolated in 26% yield from a reaction mixture containing  $[(\eta^5\text{-C}_5\text{H}_5)\text{-ZrCl}_3]$ , cycloheptatriene, magnesium, and a catalytic amount of FeCl<sub>3</sub> in a way similar to that described for the preparation of  $[(\eta^7\text{-C}_7\text{H}_7)\text{Ti}(\eta^5\text{-C}_5\text{H}_5)]$  (Scheme 2).<sup>10</sup> Purification of the air-sensitive product was achieved by means of sublimation at 140 °C and 10<sup>−2</sup> mbar, yielding dark purple crystals of **1**. As expected, the C<sub>7</sub>H<sub>7</sub> and C<sub>5</sub>H<sub>5</sub> rings in **1** give rise to only two resonance

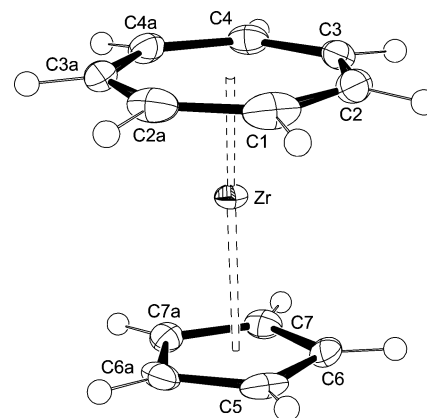


**Figure 1.** ORTEP style plot of compound **1** in the solid state. Thermal ellipsoids are drawn at the 50% probability level. Selected bond lengths (Å) and angles (deg): C1–Zr = 2.323(2), C2–Zr = 2.3295(16), C3–Zr = 2.3384(16), C4–Zr = 2.3416(15), C5–Zr = 2.494(2), C6–Zr = 2.5009(15), C7–Zr = 2.5037(15), C1–C2 = 1.423(2), C2–C3 = 1.420(2), C3–C4 = 1.418(2), C4–C4a = 1.424(2), C5–C6 = 1.410(2), C6–C7 = 1.407(2), C7–C7a = 1.408(2); C1–C2–C3 = 128.77(16), C2–C3–C4 = 128.59(15), C3–C4–C4a = 128.55(14), C2–C1–C2a = 128.17(19), C5–C6–C7 = 107.89(14), C6–C7–C7a = 108.09(13), C6–C5–C6a = 108.04(18). Symmetry operation to equivalent positions: (a)  $x, 0.5 - y, z$ .

signals in the <sup>1</sup>H and <sup>13</sup>C NMR spectra. In agreement with a previous report, the chemical shifts for the Cht and Cp hydrogen atoms (5.23 and 5.24 ppm, respectively) are almost identical, whereas the <sup>13</sup>C resonance of the C<sub>7</sub>H<sub>7</sub> ring is observed at a field (80.5 ppm) significantly higher than that of the C<sub>5</sub>H<sub>5</sub> ring (101.0 ppm).<sup>11</sup>

Since  $[(\eta^7\text{-C}_7\text{H}_7)\text{Zr}(\eta^5\text{-C}_5\text{Me}_5)]$  constitutes the only structurally characterized cycloheptatrienyl–cyclopentadienyl zirconium sandwich complex to date, the molecular structure of **1** was determined by X-ray diffraction (Figure 1). Both hydrocarbon rings are virtually planar and are coordinated in an almost perfect  $\eta^5$  (Cp) and  $\eta^7$  fashion (Cht) to the metal center. The zirconium atom and one carbon atom in each ring reside on a crystallographic mirror plane. As these two carbon atoms, C1 and C5, adopt a cis orientation, the conformation of the two rings must be regarded as being eclipsed. This situation is opposite to the staggered conformation found in the pentamethylcyclopentadienyl (Cp\*) analogue,<sup>12</sup> which otherwise exhibits very similar structural parameters. In agreement with the molecular structure of the corresponding titanium complex  $[(\eta^7\text{-C}_7\text{H}_7)\text{Ti}(\eta^5\text{-C}_5\text{H}_5)]$ ,<sup>13</sup> the metal–carbon bonds to the seven-membered ligand (2.323(2)–2.342(2) Å) are significantly shorter than those of the five-membered ring (2.494(2)–2.504(2) Å) (Table 2), revealing a much stronger interaction between the metal center and the cycloheptatrienyl ring.<sup>4</sup> Unsurprisingly, substitution of zirconium for titanium leads to considerably shorter

(7) (a) Green, M. L. H.; Walker, N. M. *J. Chem. Soc., Chem. Commun.* **1989**, 1865. (b) Diamond, G. M.; Green, M. L. H.; Mountford, P.; Walker, N. M.; Howard, J. A. K. *J. Chem. Soc., Dalton Trans.* **1992**, 417.

(8) Van Oven, H. O.; Groenenboom, C. J.; de Liefde Meijer, H. J. *J. Organomet. Chem.* **1974**, *81*, 379.

(9) Blenkers, J.; Bruin, P.; Teuben, J. H. *J. Organomet. Chem.* **1985**, *297*, 61.

(10) Demerseman, B.; Dixneuf, P. H.; Douglade, J.; Mercier, R. *Inorg. Chem.* **1982**, *21*, 3942.

(11) Groenenboom, C. J.; Jellinek, F. *J. Organomet. Chem.* **1974**, *80*, 229.

(12) Rogers, R. D.; Teuben, J. H. *J. Organomet. Chem.* **1988**, *354*, 169.

(13) Lyssenko, K. A.; Antipin, M. Y.; Ketkov, S. Y. *Russ. Chem. Bull. Int. Ed.* **2001**, *50*, 130.

metal–carbon bond lengths (Ti–C<sub>7</sub>, 2.202(1)–2.217(1) Å; Ti–C<sub>5</sub>, 2.3213(8)–2.3375(8) Å).

As the structural characterization of **1** revealed a significantly larger distance between the coplanar Cht and Cp rings in comparison with the analogous titanium structure (1.66 versus 1.49 Å and 2.20 versus 1.99 Å are determined for the distances between the metal and the centroids of the seven- and five-membered rings, respectively),<sup>13</sup> we anticipated that the interaction with additional  $\sigma$ -donor/ $\pi$ -acceptor ligands should be feasible without the requirement to open the coordination sphere by bridging the two carbocycles and distortion of the unstrained sandwich structure. In fact, addition of *tert*-butyl isocyanide (CN*t*Bu) or 2,6-dimethylphenyl isocyanide (CN-*o*-Xy) to a purple solution of **1** in THF resulted in an instantaneous color change, and the isocyanide complexes **2a** and **2b** could be isolated in almost quantitative yield as orange (for *t*BuNC) or red (for *o*-XyNC) crystals (Scheme 2). Upon coordination of the isocyanides to the zirconium atom, the resonance signals of the Cht protons in **2a** and **2b** are both shifted upfield from 5.23 ppm in **1** to 4.89 ppm, while the resonance signals of the Cp protons are shifted downfield from 5.24 ppm in **1** to 5.42 ppm in **2a** and to 5.46 ppm in **2b**, respectively. The opposite trend is observed in the <sup>13</sup>C NMR spectra of **2a** and **2b**; however, the resonances are only marginally shifted in comparison with those of **1**.

In the IR spectra, the CN stretching vibrations are at 2156 cm<sup>-1</sup> (**2a**) and 2134 cm<sup>-1</sup> (**2b**), which is only slightly shifted compared to the values for the free, uncoordinated isocyanides.<sup>14</sup> These observations indicate that metal-to-ligand  $\pi$  back-bonding in **2a** and **2b** is significantly less pronounced than in related zirconocene derivatives, in which the zirconium center is formally considered to be in the +II oxidation state. For instance,  $\nu_{\text{CN}}$  bands are found at 2027 and 1912 cm<sup>-1</sup> for the zirconocene complex [Cp<sub>2</sub>Zr(CN-*o*-Xy)]<sub>2</sub><sup>15</sup> and  $\nu_{\text{CN}}$  bands at 1995 and 1938 cm<sup>-1</sup> for the decamethylzirconocene analogue [Cp\*<sub>2</sub>Zr(CN-*o*-Xy)]<sub>2</sub>.<sup>16</sup> In mixed carbonyl–isocyanide Zr<sup>II</sup> complexes such as [Cp<sub>2</sub>Zr(CO)(CNR)], however, higher wavenumbers are observed, due to the presence of the superior  $\pi$ -acceptor CO (R = *t*Bu,  $\nu_{\text{CO}}/\nu_{\text{CN}}$  1838/2185 cm<sup>-1</sup>; R = *o*-Xy,  $\nu_{\text{CO}}/\nu_{\text{CN}}$  1842/2010 cm<sup>-1</sup>).<sup>17</sup> On the other hand, for d<sup>0</sup>-configured Zr<sup>IV</sup> complexes, even values above 2200 cm<sup>-1</sup> are found (e.g.  $\nu_{\text{CN}}$  2209 cm<sup>-1</sup> for monocationic [Cp<sub>3</sub>Zr(CN*t*Bu)]<sup>+</sup>),<sup>18</sup> whereas the *tert*-butyl isocyanide adduct of the structurally closely related cyclooctatetraenyl complex [( $\eta^8$ -C<sub>8</sub>H<sub>8</sub>)/Zr( $\eta^4$ -C<sub>8</sub>H<sub>8</sub>)] shows a CN stretching band at 2176 cm<sup>-1</sup>.<sup>19</sup> It should also be noted that considerably lower stretching frequencies are observed for related chromocene, molybdenocene, and tungstenocene derivatives. For instance,  $\nu_{\text{CN}}$  is 1835 cm<sup>-1</sup> for the tetramethyleth-

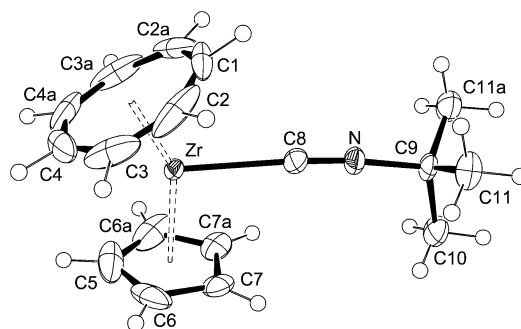


**Figure 2.** ORTEP style plot of compound **2a** in the solid state. Thermal ellipsoids are drawn at the 50% probability level. Selected bond lengths (Å) and angles (deg): C1–Zr = 2.429(3), C2–Zr = 2.375(4), C3–Zr = 2.330(3), C4–Zr = 2.386(2), C5–Zr = 2.515(3), C6–Zr = 2.527(3), C7–Zr = 2.532(2), C8–Zr = 2.376(3), C8–N = 1.150(4), N–C9 = 1.466(4), C1–C2 = 1.419(4), C2–C3 = 1.384(6), C3–C4 = 1.372(5), C4–C4a = 1.347(6), C5–C6 = 1.405(4), C6–C7 = 1.392(4), C7–C7a = 1.397(3), C9–C10 = 1.525(4), C9–C11 = 1.519(3); C1–C2–C3 = 127.3(3), C2–C3–C4 = 127.2(3), C3–C4–C4a = 130.4(3), C2–C1–C2a = 128.7(3), C5–C6–C7 = 107.4(3), C6–C7–C7a = 108.4(2), C6–C5–C6a = 108.3(3), Zr–C8–N = 175.5(2), C8–N–C9 = 174.1(3). Symmetry operation to equivalent positions: (a) *x*, *y*, 0.5 – *z*.

ylene-bridged *ansa*-chromocene [Me<sub>4</sub>C<sub>2</sub>( $\eta^5$ -C<sub>5</sub>H<sub>4</sub>)<sub>2</sub>Cr(CN*t*Bu)]<sup>20</sup> and  $\nu_{\text{CN}}$  is 1950 cm<sup>-1</sup> for the Me<sub>2</sub>Si-bridged [Me<sub>2</sub>Si( $\eta^5$ -C<sub>5</sub>Me<sub>4</sub>)<sub>2</sub>Cr(CN-*o*-Xy)].<sup>21</sup> Finally, the mono(*tert*-butyl isocyanide) complexes of molybdenocene (Cp<sub>2</sub>Mo) and tungstenocene (Cp<sub>2</sub>W) exhibit CN stretching vibrations at 1822 and 1845 cm<sup>-1</sup>, respectively.<sup>22,23</sup>

Single crystals of the *tert*-butyl isocyanide complex **2a** have been obtained from a saturated THF solution at –25 °C, and the molecular structure was determined by X-ray diffraction analysis (Figure 2). The molecule is located on a crystallographic mirror plane, which bisects the zirconium atom, the ring carbon atoms C1 and C5, and the atoms C8, N, C9, and C10 of the isocyanide ligand. Apparently, coordination of the CN*t*-Bu ligand leads to a pronounced elongation of the metal–carbon bonds: in particular, of those to the seven-membered ring (Figure 2, Table 2). The Zr–CN bond distance of 2.376(3) Å is slightly longer than has been described for cationic zirconium(IV) complexes (e.g.  $d_{\text{Zr–CN}} = 2.313(3)$  Å in [Cp<sub>3</sub>Zr(CN*t*Bu)]<sup>+</sup>),<sup>18,24</sup> but it is almost identical with the value obtained from the structural characterization of [( $\eta^8$ -C<sub>8</sub>H<sub>8</sub>)( $\eta^4$ -C<sub>8</sub>H<sub>8</sub>)Zr(CN*t*Bu)].<sup>19</sup> The Zr–C–N–C moiety is linear (Zr–C8–N = 175.5(2)°, C8–N–C9 = 174.1(3)°), and the C8–N bond length is 1.150(4) Å, which is somewhat longer than the C–N distance in the free uncoordinated isonitrile.<sup>25</sup>

(14) Stephany, R. W.; de Bie, M. J. A.; Drenth, W. *Org. Magn. Reson.* **1974**, *6*, 45. In our hands, 2,6-dimethylphenyl isocyanide shows  $\nu_{\text{CN}}$  2123 cm<sup>-1</sup> in KBr, and a THF solution of *tert*-butyl isocyanide shows a strong band at 2132 cm<sup>-1</sup>.

(15) Kool, L. B.; Rausch, M. D.; Alt, H. G.; Engelhardt, H. E.; Herberhold, M. *J. Organomet. Chem.* **1986**, *317*, C38.

(16) Wolczanski, P. T.; Bercaw, J. E. *J. Am. Chem. Soc.* **1979**, *101*, 6450. This paper quotes wavenumbers of 1795 and 1938 cm<sup>-1</sup>. Presumably, the correct figures are 1995 and 1938 cm<sup>-1</sup>.

(17) Kool, L. B.; Rausch, M. D.; Herberhold, M.; Alt, H. G.; Thewalt, U.; Honold, B. *Organometallics* **1986**, *5*, 2465.

(18) Brackemeyer, T.; Erker, G.; Fröhlich, R. *Organometallics* **1997**, *16*, 531 and references therein.

(19) Berno, P.; Floriani, C.; Chiesi-Villa, A.; Rizzoli, C. *J. Chem. Soc., Dalton Trans.* **1991**, 3085.

(20) (a) Foo, D. M.; Shapiro, P. J. *Organometallics* **1995**, *14*, 4957. (b) Matare, G. J.; Foo, D. M.; Kane, K. M.; Zehnder, R.; Wagener, M.; Shapiro, P. J.; Concolino, T.; Rheingold, A. L. *Organometallics* **2000**, *19*, 1534.

(21) Schaper, F.; Wrobel, O.; Schwörer, R.; Brintzinger, H.-H. *Organometallics* **2004**, *23*, 3552.

(22) Martins, A. M.; Calhorda, M. J.; Romão, C. C.; Völkl, C.; Kiprof, P.; Filippou, A. C. *J. Organomet. Chem.* **1992**, *423*, 367.

(23) Filippou, A. C.; Dias, A. R.; Martins, A. M.; Romão, C. C. *J. Organomet. Chem.* **1993**, *455*, 129.

(24) (a) Pflug, J.; Bertuleit, A.; Kehr, G.; Fröhlich, R.; Erker, G. *Organometallics* **1999**, *18*, 3818. (b) Ahlers, W.; Erker, G.; Fröhlich, R.; Peuchert, U. *J. Organomet. Chem.* **1999**, *578*, 115. (c) Ahlers, W.; Erker, G.; Fröhlich, R. *Eur. J. Inorg. Chem.* **1998**, 889. (d) Ahlers, W.; Erker, G.; Fröhlich, R. *J. Organomet. Chem.* **1998**, *571*, 83.



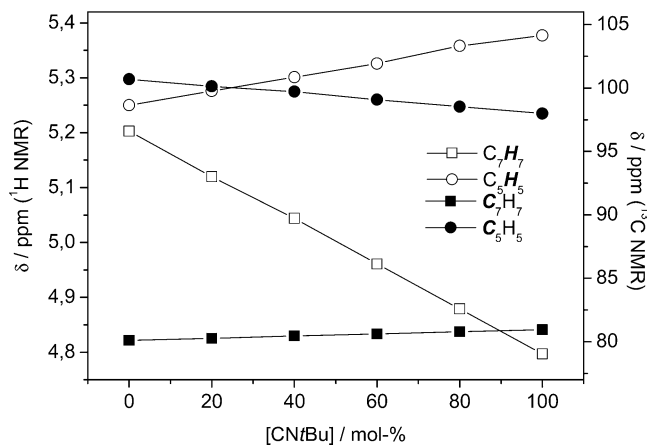


**Figure 3.** NMR titration data for the reaction of **1** with *tert*-butyl isocyanide at 20 °C.

**Dynamic NMR Studies.** For the related 16-electron chromocenes  $\text{Cp}_2\text{Cr}$  and  $\text{Cp}^*_2\text{Cr}$ , a reaction with additional ligands such as carbon monoxide leads to the formation of an equilibrium between the coordinated and uncoordinated chromocene species.<sup>26</sup> Similarly, a preliminary NMR experiment at room temperature revealed that mixtures containing **1** and substoichiometric amounts of the isocyanides showed only one set of NMR resonance signals for the  $\text{C}_7\text{H}_7$  and  $\text{C}_5\text{H}_5$  ring protons, indicating fast ligand exchange on the NMR time scale. For a 2:1 mixture of **1** and *tert*-butyl isocyanide, a variable-temperature  $^1\text{H}$  NMR study showed separate signals for **1** and **2a** below an approximate coalescence temperature of  $T_c = 233$  K, and line-shape analysis allows one to *roughly* estimate the barrier for the isocyanide coordination to about 46 kJ mol<sup>-1</sup>.<sup>27</sup> As described for the interaction of CO with decamethylmetallocenes,  $\text{Cp}^*_2\text{M}^{\text{II}}$  (M = Mg, Ca, Sr, Ba, Sm, Eu, Yb),<sup>28</sup> and for the interaction of *tert*-butyl isocyanide with decamethylcalocene,  $\text{Cp}^*_2\text{Ca}$ ,<sup>29</sup> an NMR spectroscopic investigation of the equilibrium constants  $K_C$  at various temperatures allows thermodynamic data for the equilibrium reaction of **1** with *tert*-butyl isocyanide to be established (Scheme 2). For that reason, the change of the  $^1\text{H}$  and  $^{13}\text{C}$  NMR chemical shifts for the  $\text{C}_7\text{H}_7$  and  $\text{C}_5\text{H}_5$  rings was monitored in toluene-*d*<sub>8</sub> with variation of the isocyanide concentration as well as of the temperature. As an illustrative example, Figure 3 shows the chemical shifts for the ring hydrogen and carbon resonances depending on the isocyanide concentration (0–100 mol %) at 20 °C. With increasing isocyanide concentration, the  $\text{C}_7\text{H}_7$  signals are shifted upfield from 5.20 to 4.80 ppm in the  $^1\text{H}$  NMR and downfield from 80.1 to 80.9 ppm in the  $^{13}\text{C}$  NMR

(25) Allen, F. H.; Kennard, O.; Watson, D. G.; Brammer, L.; Orpen, G. A.; Taylor, R. *J. Chem. Soc., Perkin Trans. 2* **1987**, S1.

(26) (a) Tang Wong, K. L.; Brintzinger, H.-H. *J. Am. Chem. Soc.* **1975**, *97*, 5143. (b) Van Raaij, E. U.; Brintzinger, H. H. *J. Organomet. Chem.* **1988**, *356*, 315. (c) Schaper, F.; Rentzsch, M.; Prosenk, M.-H.; Rief, U.; Schmidt, K.; Brintzinger, H.-H. *J. Organomet. Chem.* **1997**, *534*, 67.

(27) The following approximate equation was used for the calculation of  $\Delta G^\ddagger$ :  $\Delta G^\ddagger = 4.57T_c(22.96 + \ln(T/\Delta\nu))$  (J/mol) with  $T_c = 233$  K and  $\Delta\nu = 127$  Hz, according to: Günther, H. *NMR Spectroscopy*; Georg Thieme Verlag: Stuttgart, Germany, 1973; p 248.

(28) (a) Selg, P.; Brintzinger, H. H.; Anderson, R. A.; Horváth, I. T. *Angew. Chem.* **1995**, *107*, 877; *Angew. Chem., Int. Ed. Engl.* **1995**, *34*, 791. (b) Selg, P.; Brintzinger, H. H.; Schultz, M.; Andersen, R. A. *Organometallics* **2002**, *21*, 3100.

(29) Selg, P. Dissertation, Universität Konstanz, 1996.

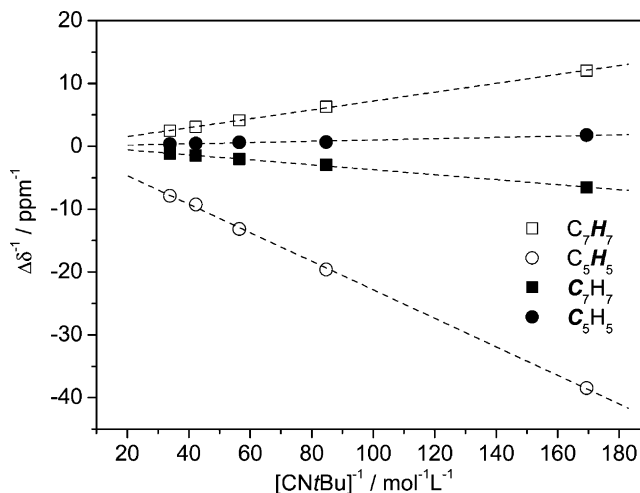


**Figure 4.** Benesi–Hildebrand treatment of the NMR titration data for the reaction of **1** with *tert*-butyl isocyanide at 20 °C.

spectra, while at the same time the  $\text{C}_5\text{H}_5$  signals shift only slightly upfield from 5.25 to 5.38 ppm in the proton, and downfield from 100.7 to 98.0 ppm in the carbon NMR spectra. Adding more than 1 equiv of isocyanide to the reaction mixture does not further result in a significant shifting of the NMR signals, indicating that coordination of a second ligand molecule to the zirconium isocyanide complex **2a** is unlikely to take place under these conditions. Due to the fact that the change of the chemical shifts  $\Delta\delta$  is a linear function of the mole fractions of the uncoordinated sandwich compound **1** and the isocyanide complex **2a**, the equilibrium constants  $K_C$  can be obtained by plotting the reciprocal of  $\Delta\delta$  against the reciprocal of the isocyanide concentration  $[\text{CNtBu}]^{-1}$ ,<sup>28,29</sup> which is expected to give a straight line with a slope  $(K_C\Delta\delta_{\text{max}})^{-1}$  and an intercept  $(\Delta\delta_{\text{max}})^{-1}$  for the formation of a *mono*isocyanide complex. However, this method, which represents an NMR adaptation<sup>30</sup> of the Benesi–Hildebrand treatment originally used in optical spectroscopy studies,<sup>31</sup> can only be applied at temperatures above the coalescence temperature  $T_c = 233$  K. The values for  $K_C$  at 213 and 193 K, on the other hand, were determined directly by integration of the  $^1\text{H}$  NMR  $\text{C}_7\text{H}_7$  and  $\text{C}_5\text{H}_5$  resonances of **1** and **2a**. For illustration, Figure 4 shows the Benesi–Hildebrand plots at 293 K, and the values for  $K_C$  are assembled in Table 1.

Thermodynamic data for the complex formation reaction can be obtained from a van't Hoff plot of  $\ln K_C$  vs  $1/T$ , and the standard reaction enthalpy and entropy changes are determined from the slope ( $\Delta H^\circ/R$ ) and from the intercept ( $\Delta S^\circ/R$ ).<sup>32</sup> In addition, the free energy change  $\Delta G^\circ$  is calculated by application of the Gibbs–Helmholtz equation (Table 1). The thermodynamic data obtained from monitoring the different resonance signals are all in the same order of magnitude, indicating that the reaction is slightly exergonic with an average value of  $\Delta G^\circ = -0.85 \pm 0.54$  kJ mol<sup>-1</sup>. The average standard enthalpy of complex formation and the associ-

(30) Fielding, L. *Tetrahedron* **2000**, *56*, 6151.

(31) Benesi, H. A.; Hildebrand, J. H. *J. Am. Chem. Soc.* **1949**, *71*, 2703.

(32) The average values and errors were calculated by linear least-squares regression analysis.

**Table 1. Thermodynamic Data for the Reaction of ( $\eta^7$ -C<sub>7</sub>H<sub>7</sub>)Zr( $\eta^5$ -C<sub>5</sub>H<sub>5</sub>) (**2**) with CN*t*Bu<sup>a</sup>**

temp (K)	<i>K</i> (M <sup>-1</sup> )			
	C <sub>7</sub> H <sub>7</sub>	C <sub>5</sub> H <sub>5</sub>	C <sub>7</sub> H <sub>7</sub>	C <sub>5</sub> H <sub>5</sub>
193 <sup>b</sup>	4804 ± 3560	3018 ± 1620		
213 <sup>b</sup>	3652 ± 2335	2818 ± 1287		
253 <sup>c</sup>	18.6 ± 10.9	17.6 ± 10.0	17.8 ± 10.8	17.9 ± 15.0
273 <sup>c</sup>	5.3 ± 2.4	3.9 ± 1.2	5.0 ± 5.4	3.4 ± 0.7
293 <sup>c</sup>	1.9 ± 1.3	0.5 ± 1.3	1.1 ± 1.3	2.5 ± 0.8
$\Delta H^\circ$ (kJ mol <sup>-1</sup> ) <sup>d</sup>	-40.8 ± 5.15	-43.3 ± 6.15	-43.2 ± 4.1	-30.9 ± 11.0
$\Delta S^\circ$ (J mol <sup>-1</sup> K <sup>-1</sup> ) <sup>e</sup>	-134 ± 21.8	-149 ± 26.0	-146 ± 15.1	-99.6 ± 40.3
$\Delta G^\circ$ (298 K) (kJ mol <sup>-1</sup> ) <sup>f</sup>	-0.86 ± 0.25	-1.00 ± 0.29	-0.35 ± 0.70	-1.20 ± 0.91

<sup>a</sup> The data were obtained by monitoring the C<sub>7</sub>H<sub>7</sub> and C<sub>5</sub>H<sub>5</sub> <sup>1</sup>H and <sup>13</sup>C NMR resonances; the respective resonance is marked in italics. <sup>b</sup> *K*<sub>C</sub> was determined by integration of the C<sub>7</sub>H<sub>7</sub> and C<sub>5</sub>H<sub>5</sub> <sup>1</sup>H NMR resonances of **1** and **2a** with respect to the integral of the toluene signal at  $\delta$  2.09 ppm with *K*<sub>C</sub> = [**2a**]/[**1**][CN*t*Bu]; integration of the <sup>13</sup>C NMR resonances did not produce reasonable results. <sup>c</sup> *K*<sub>C</sub> was calculated from the slope and intercept of  $\Delta\delta^{-1}$  against [CN*t*Bu]<sup>-1</sup> with  $\Delta\delta^{-1} = (K_C \Delta\delta_{\max})^{-1}[\text{CN}t\text{Bu}]^{-1} + \Delta\delta_{\max}^{-1}$ . <sup>d</sup> Calculated from the slope of ln *K*<sub>C</sub> against *T*<sup>-1</sup> with ln *K*<sub>C</sub> =  $-(\Delta H^\circ/R)T^{-1} + (\Delta S^\circ/R)$ ; *R* = 8.3145 J mol<sup>-1</sup> K<sup>-1</sup>. <sup>e</sup> Calculated from the intercept of *T*<sup>-1</sup> against ln *K*<sub>C</sub> with ln *K*<sub>C</sub> =  $-(\Delta H^\circ/R)T^{-1} + (\Delta S^\circ/R)$ ; *R* = 8.3145 J mol<sup>-1</sup> K<sup>-1</sup>. <sup>f</sup> Calculated from  $\Delta G^\circ = \Delta H^\circ - T\Delta S^\circ$  at 298 K.

ated entropy change amount to  $\Delta H^\circ = -39.6 \pm 6.6$  kJ mol<sup>-1</sup> and  $\Delta S^\circ = -132.2 \pm 25.8$  J mol<sup>-1</sup> K<sup>-1</sup>, respectively. For related reactions involving carbon monoxide and the 16-electron triplet species vanadocene iodide (Cp<sub>2</sub>VI) and chromocene (Cp<sub>2</sub>Cr), the following thermodynamic quantities have been obtained:  $\Delta H^\circ = -54.8 \pm 4.2$  kJ mol<sup>-1</sup> and  $\Delta S^\circ = -144.8 \pm 14.2$  J mol<sup>-1</sup> K<sup>-1</sup> for the formation of [Cp<sub>2</sub>V(CO)I],<sup>33</sup>  $\Delta H^\circ = -78.7 \pm 2.1$  kJ mol<sup>-1</sup> and  $\Delta S^\circ = -251.0 \pm 8.4$  J mol<sup>-1</sup> K<sup>-1</sup> for the formation of [Cp<sub>2</sub>Cr(CO)].<sup>26a</sup> The latter values are in good agreement with theoretical calculations, which estimated the bond dissociation energy (BDE) for the loss of CO from [Cp<sub>2</sub>Cr(CO)] as 76.4 kJ mol<sup>-1</sup>.<sup>34</sup> It should be noted that significantly higher values have been calculated for the dissociation of CO from the corresponding molybdenocene (BDE = 163.6 kJ mol<sup>-1</sup>) and tungstenocene (172.1 kJ mol<sup>-1</sup>),<sup>33,34</sup> which already falls in the range of experimentally derived bond dissociation enthalpies in homoleptic transition-metal carbonyls such as M(CO)<sub>6</sub> (M = Cr, Mo, W).<sup>35</sup> In contrast to these transition-metal complexes, CO adducts of main-group-element and lanthanide metallocenes of the type [Cp\*<sub>2</sub>M(CO)] (M = Ca, Eu, Yb) are considerably more labile. For instance,  $\Delta H^\circ = -17.1 \pm 1.9$  kJ mol<sup>-1</sup> and  $\Delta S^\circ = -85.2 \pm 6.8$  J mol<sup>-1</sup> K<sup>-1</sup> for the reversible reaction of decamethylcalocene with CO.<sup>28b</sup> Unfortunately, no thermodynamic data have been reported for the reaction of Cp\*<sub>2</sub>Ca with *tert*-butyl isocyanide.<sup>29</sup>

In agreement with the small propensity of the 16-electron [1]silatroticenophane **1** to form a stable carbonyl complex (Figure 1), the standard enthalpy of  $\Delta H^\circ = -39.6 \pm 6.6$  kJ mol<sup>-1</sup> for the formation of complex **2a**

(33) Calderazzo, F.; Fachinetti, G.; Floriani, C. *J. Am. Chem. Soc.* **1974**, *96*, 3695.

(34) Green, J. C.; Jardine, C. N. *J. Chem. Soc., Dalton Trans.* **1999**, 3767. It should be noted that  $\Delta S^\circ$  for the reversible binding of CO to Cp<sub>2</sub>Cr has been quoted incorrectly.<sup>26a</sup>

(35) (a) Martinho Simões, J. A.; Beauchamp, J. L. *Chem. Rev.* **1990**, *90*, 629. (b) Pilcher, G.; Skinner, H. A. In *The Chemistry of the Metal–Carbon Bond*; Hartley, F. R.; Patai, S., Eds.; Wiley: Oxford, U.K., 1982; p 43.

indicates a rather weak zirconium–isocyanide bond in comparison with “conventional” transition-metal isocyanide complexes. For instance, the enthalpy for the reaction of *tert*-butyl isocyanide with dimeric [Rh(I)-(PiPr<sub>3</sub>)<sub>2</sub>Cl]<sub>2</sub> has been determined by means of calorimetric measurements to be  $\Delta H^\circ = -140.2 \pm 2.1$  kJ mol<sup>-1</sup>, which results in a lower limit of 177.4 kJ mol<sup>-1</sup> for the Rh–isocyanide bond dissociation energy (BDE).<sup>36</sup> Similar values have been obtained for the strength of the molybdenum–isocyanide bonds by studying ligand exchange reactions for [L<sub>3</sub>Mo(CO)<sub>3</sub>] complexes.<sup>37</sup>

**Theoretical Studies.** For a more detailed insight into the electronic structure, bonding, and reactivity of mixed Cht–Cp zirconium sandwich complexes, additional theoretical calculations have been carried out on the 16-electron complex **1** as well as on the isocyanide complexes **2a** and **2b**. The calculations were performed using the *Gaussian03* package.<sup>38</sup> All structures were fully optimized on the density functional theory (DFT) level employing the B3LYP hybrid functional.<sup>39</sup> For all main-group elements (C, H and N) the all-electron triple- $\zeta$  basis set (6-311G\*\*) was used, whereas for the group 4 transition metal Zr a small-core relativistic ECP together with the corresponding triple- $\zeta$  valence basis set was employed (*Stuttgart RSC 1997 ECP*).<sup>40,41</sup> The optimized structural parameters for all compounds are in good agreement with the values established by X-ray crystallography (Table 2).<sup>42</sup>

For complex **1**, contour plots of relevant molecular orbitals involving contributions from the C<sub>7</sub>H<sub>7</sub> and C<sub>5</sub>H<sub>5</sub>  $\pi$  molecular orbitals together with their eigenvalues are given in Figure 5. In agreement with other theoretical and experimental investigations of the bonding in mixed

(36) Wang, K.; Rosini, G. P.; Nolan, S. P.; Goldman, A. S. *J. Am. Chem. Soc.* **1995**, *117*, 5082.

(37) Nolan, S. P.; Lopez de la Vega, R.; Hoff, C. D. *Organometallics* **1986**, *5*, 2529.

(38) Frisch, M. J.; Trucks, G. W.; Schlegel, H. B.; Scuseria, G. E.; Robb, M. A.; Cheeseman, J. R.; Montgomery, Jr., J. A.; Vreven, T.; Kudin, K. N.; Burant, J. C.; Millam, J. M.; Iyengar, S. S.; Tomasi, J.; Barone, V.; Mennucci, B.; Cossi, M.; Scalmani, G.; Rega, N.; Petersson, G. A.; Nakatsuji, H.; Hada, M.; Ehara, M.; Toyota, K.; Fukuda, R.; Hasegawa, J.; Ishida, M.; Nakajima, T.; Honda, Y.; Kitao, O.; Nakai, H.; Klene, M.; Li, X.; Knox, J. E.; Hratchian, H. P.; Cross, J. B.; Bakken, V.; Adamo, C.; Jaramillo, J.; Gomperts, R.; Stratmann, R. E.; Yazyev, O.; Austin, A. J.; Cammi, R.; Pomelli, C.; Ochterski, J. W.; Ayala, P. Y.; Morokuma, K.; Voth, G. A.; Salvador, P.; Dannenberg, J. J.; Zakrzewski, V. G.; Dapprich, S.; Daniels, A. D.; Strain, M. C.; Farkas, O.; Malick, D. K.; Rabuck, A. D.; Raghavachari, K.; Foresman, J. B.; Ortiz, J. V.; Cui, Q.; Baboul, A. G.; Clifford, S.; Cioslowski, J.; Stefanov, B. B.; Liu, G.; Liashenko, A.; Piskorz, P.; Komaromi, I.; Martin, R. L.; Fox, D. J.; Keith, T.; Al-Laham, M. A.; Peng, C. Y.; Nanayakkara, A.; Challacombe, M.; Gill, P. M. W.; Johnson, B.; Chen, W.; Wong, M. W.; Gonzalez, C.; Pople, J. A. *Gaussian 03*, Revision C.02; Gaussian, Inc., Wallingford, CT, 2004.

(39) (a) Becke, A. D. *J. Chem. Phys.* **1993**, *98*, 5648. (b) Miehlich, B.; Savin, A.; Stoll, H.; Preuss, H. *Chem. Phys. Lett.* **1989**, *157*, 200. (c) Lee, C.; Yang, W.; Parr, G. *Phys. Rev. B* **1988**, *37*, 785.

(40) Dolg, M.; Stoll, H.; Preuss, H.; Pitzer, R. M. *J. Phys. Chem.* **1993**, *97*, 5852.

(41) Basis sets were obtained from the Extensible Computational Chemistry Environment Basis Set Database, Version 02/25/04 (<http://www.emsl.pnl.gov/forms/basisform.html>), as developed and distributed by the Molecular Science Computing Facility, Environmental and Molecular Sciences Laboratory, which is part of the Pacific Northwest Laboratory, P.O. Box 999, Richland, WA 99352, and funded by the U.S. Department of Energy. The Pacific Northwest Laboratory is a multiprogram laboratory operated by Battelle Memorial Institute for the U.S. Department of Energy under Contract No. DE-AC06-76RLO 1830. Contact David Feller or Karen Schuchardt for further information.

(42) Presentations of the calculated molecular structures of **1**, **2a**, and **2b** as well as of the isocyanides *t*BuNC and *o*-XyNC together with Cartesian coordinates of their atomic positions can be found in the Supporting Information.

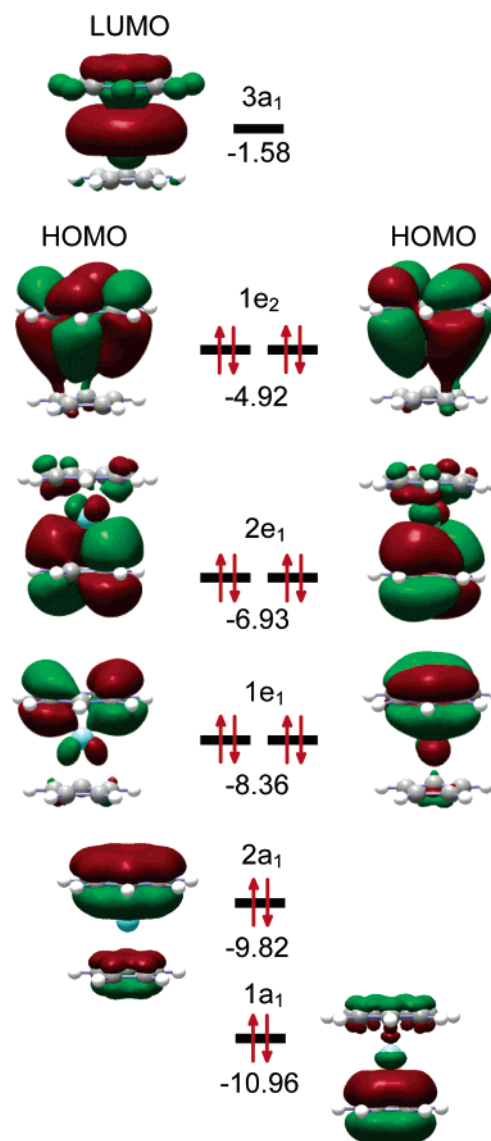
**Table 2.** Comparison of Experimentally and Theoretically Derived Structural Parameters<sup>a</sup> of **1**, **2a**, and **2b**

	<b>1</b>		<b>2a</b>		<b>2b</b>
	X-ray	DFT	X-ray	DFT	DFT
Zr–C <sub>cht</sub> <sup>b</sup>	1.66	1.71	1.75	1.80	1.82
Zr–C <sub>cht</sub>					
av	2.335(2)	2.371	2.373(3)	2.434	2.441
range	2.323(2)–2.342(2)	2.369–2.375	2.330(3)–2.429(3)	2.374–2.505	2.378–2.506
C <sub>cht</sub> –C <sub>cht</sub>					
av	1.421(2)	1.426	1.385(5)	1.422	1.421
range	1.418(2)–1.424(2)	1.421–1.432	1.347(6)–1.419(4)	1.404–1.433	1.397–1.435
Zr–C <sub>cp</sub> <sup>c</sup>	2.20	2.24	2.23	2.28	2.27
Zr–C <sub>cp</sub>					
av	2.500(2)	2.550	2.527(3)	2.578	2.574
range	2.494(2)–2.504(2)	2.547–2.552	2.515(3)–2.532(2)	2.574–2.582	2.562–2.587
C <sub>cp</sub> –C <sub>cp</sub>					
av	1.408(2)	1.418	1.398(4)	1.418	1.417
range	1.407(2)–1.410(2)	1.415–1.423	1.392(4)–1.405(4)	1.416–1.420	1.412–1.422
C <sub>cht</sub> –Zr–C <sub>cp</sub>	175.6	180.0	149.4	149.2	148.6
Zr–CN			2.376(3)	2.378	2.355
C–N			1.150(4)	1.172	1.178
Zr–C–N			175.5(2)	177.6	179.3
C–N–R			174.1(3)	177.2	179.4

<sup>a</sup> Bond lengths in Å and angles in deg. <sup>b</sup> C<sub>cht</sub> = centroid of the seven-membered ring; C<sub>cht</sub> = carbon atom of the seven-membered ring. <sup>c</sup> C<sub>cp</sub> = centroid of the five-membered ring; C<sub>cp</sub> = carbon atom of the five-membered ring.

Cht–Cp sandwich molecules,<sup>5,43,44</sup> the LUMO in **1** is essentially metal localized and consists of the 4d<sub>2</sub><sup>2</sup> orbital with a small contribution from the C<sub>7</sub>H<sub>7</sub> a<sub>1</sub> molecular orbital, in a coordinate system in which the metal–ring axis is defined as the z axis. The degenerate set of the highest occupied molecular orbitals (1e<sub>2</sub>)<sup>45</sup> stems from δ bonding between the metal and the cycloheptatrienyl ring, and a strong contribution from both zirconium and C<sub>7</sub>H<sub>7</sub> e<sub>2</sub> MOs indicates a significant degree of covalency.<sup>43</sup> The next two levels represent the π bonds to the cyclopentadienyl ring (2e<sub>1</sub>)<sup>45</sup> and to the cycloheptatrienyl ring (1e<sub>1</sub>),<sup>45</sup> respectively. Since the 2e<sub>1</sub> molecular orbitals are made up predominantly of the C<sub>5</sub>H<sub>5</sub> e<sub>1</sub> orbitals, it can be concluded that the interaction between the metal and the Cp ring can be regarded as being largely ionic.<sup>43</sup> In addition, those molecular orbitals, HOMO-13 (2a<sub>1</sub>)<sup>45</sup> and HOMO-18 (1a<sub>1</sub>),<sup>45</sup> are shown which exhibit contributions from the C<sub>7</sub>H<sub>7</sub> and C<sub>5</sub>H<sub>5</sub> π molecular orbitals of a<sub>1</sub> symmetry.

Naturally, coordination of an additional two-electron-donor ligand to complex **1** requires bending of the two carbocycles (Figure 2). In a fashion similar to that described for the frontier orbitals in the [1]silatroticenophane **I**,<sup>4</sup> this bending and distortion of the sandwich structure from an idealized C<sub>∞v</sub> toward a C<sub>s</sub> symmetric orientation leads to a LUMO of a' symmetry and a HOMO of a'' symmetry, which are suitably oriented for σ and π interaction with one additional ligand. For illustration, a single-point calculation was performed for the frozen Cht–Cp–Zr fragment in **2a**, and the resulting frontier orbitals (LUMO, HOMO, and HOMO-1) and their energies are shown in Figure 6. In fact, coordination of *tert*-butyl isocyanide (a σ-donor/π-

**Figure 5.** Contour plots and eigenvalues (in eV) of relevant molecular orbitals in **1**.

(43) (a) Menconi, G.; Kaltsoyannis, N. *Organometallics* **2005**, *24*, 1189. (b) Kaltsoyannis, N. *J. Chem. Soc., Dalton Trans.* **1995**, 3727.

(44) (a) Green, J. C.; Kaltsoyannis, N.; Sze, K. H.; MacDonald, M. *J. Am. Chem. Soc.* **1994**, *116*, 1994. (b) Green, J. C.; Green, M. L. H.; Kaltsoyannis, N.; Mountford, P.; Scott, P.; Simpson, S. *J. Organometallics* **1992**, *11*, 3353. (c) Groenenboom, C. J.; de Liefde Meijer, H. J. *J. Organomet. Chem.* **1975**, *97*, 73. (d) Evans, S.; Green, J. C.; Jackson, S. E.; Higginson, B. *J. Chem. Soc., Dalton Trans.* **1974**, 304.

(45) These symmetry labels refer to the idealized point group C<sub>∞v</sub>, in which infinite axes of rotation are assumed for the carbocyclic rings.



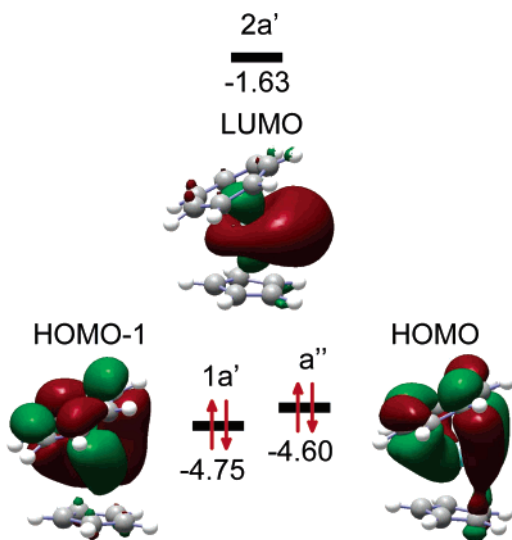


**Figure 6.** Contour plots and eigenvalues (in eV) of the valence molecular orbitals in the frozen Cht–Cpt–Zr fragment in **2a**.

acceptor ligand) and formation of **2a** were experimentally found to be exothermic by  $\Delta H^\circ = -39.6 \pm 6.6$  kJ mol<sup>-1</sup> (vide supra), a value which is in good agreement with the calculated enthalpy of formation of  $\Delta H^\circ = -36.5$  kJ mol<sup>-1</sup>.<sup>46</sup> Examination of the molecular orbitals in **2a** clearly reveals that  $\sigma$  donation from the *t*BuNC ligand represents the main contribution to the stabilization of the isocyanide complex **2a**. This  $\sigma$  bond, however, *cannot* be explained in terms of a simple two-orbital interaction between the HOMO of the isocyanide and the LUMO of the Cht–Cp–Zr complex fragment, since it does also involve additional Cht- and Cp-localized molecular orbitals of *a'* symmetry. Accordingly, we refrain from making an attempt to comprehensively represent these orbital interactions.

In contrast, a relatively simple picture can be drawn for  $\pi$  back-donation to the *t*BuNC ligand by analysis of the two highest-occupied molecular orbitals in **2a** (Figure 7, top). Apparently, HOMO-1 in **2a** can be regarded as the bonding linear combination of the isocyanide *a''* LUMO with the *a''* HOMO of the bent Cht–Cp–Zr complex fragment. Although visual inspection of the shape of the resulting molecular orbital suggests the presence of only slight  $\pi$  overlap, this interaction accounts for the stabilization of the *a''* orbital with respect to the corresponding *a'* orbital, which is not involved in isocyanide bonding and turns into the HOMO of **2a** (Figure 6 and Figure 7, top). Furthermore,  $\pi$  interaction is also responsible for the theoretical as well as experimental<sup>47</sup> observation that the 2,6-dimethylphenyl isocyanide ligand in **2b** adopts a vertical conformation with a coplanar orientation toward the

mirror plane including zirconium and the centroids of the Cht and Cp rings. As was also described for bis-(cyclopentadienyl)–ML<sub>*n*</sub> complexes,<sup>48</sup> this orientation is electronically more favorable, since it allows the alignment of the LUMO of the isocyanide ligand in an antisymmetric fashion with respect to the mirror plane in order to interact optimally with the *a''* HOMO of the Cht–Cp–Zr complex fragment (Figure 7, bottom).<sup>49</sup> Theoretically, the presence of  $\pi$  back-donation is also uncovered by comparison of the calculated CN stretching frequencies for the free and for the coordinated isocyanide ligands in **2a** and **2b** (Table 3). Upon complexation, a shift to lower wavenumbers is observed, which is less pronounced for the aliphatic *t*BuNC ( $\Delta\nu = -21$  cm<sup>-1</sup>) than for the aromatic *o*-XyNC ligand ( $\Delta\nu = -43$  cm<sup>-1</sup>). This trend is not in agreement with the results of the experimental IR spectroscopic investigation (Table 3); both experimental and theoretical values, however, are consistent with only weak  $\pi$  back-donation from the Cht–Cp–Zr fragment. Finally, the different  $\sigma$ -donor/ $\pi$ -acceptor characteristics of the isocyanides in **2a** and **2b** do not significantly affect the relative stability of the two isocyanide complexes, and an enthalpy of  $\Delta H^\circ = -38.2$  kJ mol<sup>-1</sup> is calculated for the formation of **2b**,<sup>46</sup> which is very similar to the value obtained theoretically ( $\Delta H^\circ = -36.5$  kJ mol<sup>-1</sup>) and experimentally ( $\Delta H^\circ = -39.6 \pm 6.6$  kJ mol<sup>-1</sup>) for the formation of **2a** (Table 3).

### 3. Conclusion

In this contribution, we have studied the reactivity of the cycloheptatrienyl–cyclopentadienyl–zirconium sandwich complex [( $\eta^7$ -C<sub>7</sub>H<sub>7</sub>)Zr( $\eta^5$ -C<sub>5</sub>H<sub>5</sub>)] (**1**) toward alkyl and aryl isocyanides. Both experimental and theoretical results suggest that the zirconium–isocyanide interaction in the resulting complexes [( $\eta^7$ -C<sub>7</sub>H<sub>7</sub>)( $\eta^5$ -C<sub>5</sub>H<sub>5</sub>)Zr(CNR)] (R = *t*Bu, **2a**; R = **2b**, *o*-Xy) is relatively weak and that the 16-electron complex **1** has only a small propensity to efficiently interact with  $\sigma$ -donor/ $\pi$ -acceptor ligands. In this respect, **1** does not act like a complex containing zirconium in a lower oxidation state but rather bears a closer resemblance to Lewis acidic Zr<sup>IV</sup> complexes. On the basis of the theoretical calculations, this behavior can be mainly attributed to the strong and appreciably covalent zirconium–cycloheptatrienyl interaction, leading to highly stabilized frontier orbitals and consequently to a diminishing  $\pi$ -electron release capability. This interpretation is also supported by a recent investigation of the bonding in [( $\eta^7$ -C<sub>7</sub>H<sub>7</sub>)M( $\eta^5$ -C<sub>5</sub>H<sub>5</sub>)] (M = groups 4–6), which resulted in the conclusion “that the cycloheptatrienyl ring functions more as a –3 ligand than as a +1 ligand in these mixed ring complexes”,<sup>43a</sup> a description which was also found to be valid for cycloheptatrienyl sandwich compounds of actinides.<sup>52</sup>

### 4. Experimental Section

All operations were performed under an atmosphere of dry argon by using Schlenk and vacuum techniques. Solvents were

(46) The reaction enthalpy for the formation of the isocyanide complexes **2a** and **2b** was calculated by subtracting the energies of the ground-state electronic structures of **1** and the respective isocyanide from that of the corresponding isocyanide complex.

(47) A vertical conformation can clearly be deduced from the crystal structure analysis of compound **2b**: C<sub>21</sub>H<sub>21</sub>NZr, *M<sub>r</sub>* = 378.61, red needle (0.13 × 0.20 × 0.38 mm<sup>3</sup>), monoclinic, *P*2<sub>1</sub> (No. 4), *a* = 10.9010(5) Å, *b* = 6.8109(3) Å, *c* = 11.6271(8) Å,  $\beta$  = 101.769(2)°, *V* = 845.11(8) Å<sup>3</sup>, *Z* = 2, *d*<sub>calcd</sub> = 1.488 g cm<sup>-3</sup>, *F*<sub>000</sub> = 388,  $\mu$  = 0.649 mm<sup>-1</sup>. Unfortunately, an unresolvable disorder of the cyclopentadienyl ring and dubious thermal displacement parameters of the cycloheptatrienyl ring preclude a satisfactory structure solution (R1 = 0.0386 (*I<sub>o</sub>* > 2σ(*I<sub>o</sub>*)), wR2 = 0.0805 (all data), GOF = 1.056).

(48) (a) Lauder, J. W.; Hoffmann, R. *J. Am. Chem. Soc.* **1976**, *98*, 1729. (b) Green, J. C. *Chem. Soc. Rev.* **1998**, 263.

(49) A presentation of the frontier orbitals in 2,6-dimethylphenyl isocyanide can be found in the Supporting Information.

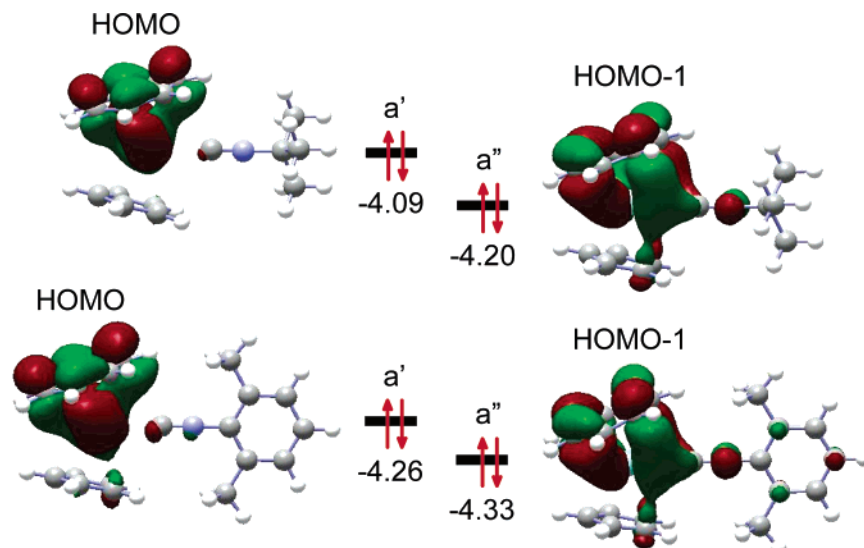


**Figure 7.** Contour plots and eigenvalues (in eV) of the valence molecular orbitals in **2a** (top) and **2b** (bottom).

**Table 3. Comparison of Selected Experimental and Theoretical Data for Complexes 2a and 2b**

	$\nu(\text{CN})$ ( $\text{cm}^{-1}$ )		$\Delta H^\circ(\text{Zr}-\text{CNR})$ ( $\text{kJ mol}^{-1}$ )	
	exptl	DFT	exptl	DFT
<i>t</i> BuNC	2132	2206		
<b>2a</b>	2156	2185	$-39.6 \pm 6.6$	-36.5
<i>o</i> -XyNC	2123	2184		
<b>2b</b>	2134	2141		-38.2

dried by standard methods and distilled prior to use.  $\text{CpZrCl}_3$  has been prepared from  $\text{Cp}_2\text{ZrCl}_2$  and  $\text{ZrCl}_4$  according to published procedures.<sup>50</sup> Elemental analyses (C, H, N) were performed on an Elementar Vario EL elemental analyzer.  $^1\text{H}$  NMR and  $^{13}\text{C}$  NMR spectra were measured on JEOL JNM GX 270, JEOL JNM GX 400, and Bruker DPX 400 spectrometers using the solvent as internal standard. IR spectra were recorded on a Bio-Rad FTS 575C instrument.

**[( $\eta^7\text{-C}_7\text{H}_7$ )Zr( $\eta^5\text{-C}_5\text{H}_5$ )] (1).** The synthesis was performed in a fashion similar to that described for  $[(\eta^7\text{-C}_7\text{H}_7)\text{Ti}(\eta^5\text{-C}_5\text{H}_5)]$ .<sup>5</sup> A Schlenk flask was charged with magnesium turnings (2.17 g, 89.3 mmol), catalytic amounts of ferric chloride (0.2 g, 1.23 mmol), freshly distilled cycloheptatriene (5.5 mL, 4.89 g, 53.1 mmol), and THF (10 mL). This reaction mixture was treated dropwise with a solution of  $\text{CpZrCl}_3$  (6.5 g, 24.75 mmol) in THF (50 mL) over a period of 1 h. After the mixture was stirred overnight at room temperature, all volatiles were removed in vacuo. The air-sensitive residue was sublimed at  $140^\circ\text{C}$  and  $10^{-2}$  mbar to obtain 1.6 g (6.47 mmol; 26%) of  $[(\text{C}_7\text{H}_7)\text{Zr}(\text{C}_5\text{H}_5)]$  (**1**) as a purple crystalline solid.  $^1\text{H}$  NMR (400 MHz, benzene- $d_6$ ):  $\delta$  5.24 (s, 5H,  $\text{C}_5\text{H}_5$ ), 5.23 (s, 7H,  $\text{C}_7\text{H}_7$ ).  $^{13}\text{C}$  NMR (400 MHz, benzene- $d_6$ ):  $\delta$  101.0 ( $\text{C}_5\text{H}_5$ ), 80.5 ( $\text{C}_7\text{H}_7$ ). Full characterization of **1**, including an accurate elemental analysis, has been reported previously.<sup>8</sup>

**[( $\eta^7\text{-C}_7\text{H}_7$ )Zr( $\eta^5\text{-C}_5\text{H}_5$ )Zr(CN*t*Bu)] (2a).** To a solution of  $[(\eta^7\text{-C}_7\text{H}_7)\text{Zr}(\eta^5\text{-C}_5\text{H}_5)]$  (200 mg, 0.81 mmol) in THF (20 mL) was added a solution of *tert*-butyl isocyanide (67.2 mg, 0.81 mmol)

in THF (10 mL). Upon addition, an instantaneous color change from purple to orange was observed. The solution was stirred for 15 min and evaporated to dryness, yielding  $[(\text{C}_7\text{H}_7)\text{Zr}(\text{C}_5\text{H}_5)(\text{CN}i\text{tBu})]$  (**2a**) as an orange solid (254 mg, 0.77 mmol, 95% yield). Single crystals were obtained by cooling a saturated THF solution to  $-25^\circ\text{C}$ . Anal. Calcd for  $\text{C}_{17}\text{H}_{21}\text{NZr}$  (330.57): C, 61.77; H, 6.40; N, 4.24. Found: C, 60.29; H, 6.32; N, 3.96.  $^1\text{H}$  NMR (400 MHz, benzene- $d_6$ ):  $\delta$  5.42 (s, 5H,  $\text{C}_5\text{H}_5$ ), 4.89 (s, 7H,  $\text{C}_7\text{H}_7$ ), 0.68 (t, 9H,  $\text{CCH}_3$ ).  $^{13}\text{C}$  NMR (100.53 MHz, benzene- $d_6$ ):  $\delta$  148.0 (CNR), 98.3 ( $\text{C}_5\text{H}_5$ ), 81.3 ( $\text{C}_7\text{H}_7$ ), 55.3 ( $\text{CCH}_3$ ), 29.2 ( $\text{CCH}_3$ ). IR (KBr):  $\nu$  2156  $\text{cm}^{-1}$  ( $\text{C}\equiv\text{N}$ ). We assume that the elemental analyses are unsatisfactory due to partial loss and evaporation of the isocyanide ligand upon drying the crystals in vacuo.

**[( $\eta^7\text{-C}_7\text{H}_7$ )Zr( $\eta^5\text{-C}_5\text{H}_5$ )Zr(CN-*o*-Xy)] (2b).** A solution of  $[(\eta^7\text{-C}_7\text{H}_7)\text{Zr}(\eta^5\text{-C}_5\text{H}_5)]$  (250 mg, 1.01 mmol) in THF (25 mL) was treated with a solution of 2,6-dimethylphenyl isocyanide (133 mg, 1.01 mmol) in THF (15 mL). Upon addition, the purple solution turned red. After it was stirred for 15 min, the reaction mixture was evaporated to dryness, yielding  $[(\text{C}_7\text{H}_7)\text{Zr}(\text{C}_5\text{H}_5)(\text{CN-}o\text{-Xy})]$  (**2b**) as a red solid (371 mg, 0.98 mmol, 97% yield), which can be purified by recrystallization from a THF solution at  $-25^\circ\text{C}$ . Anal. Calcd for  $\text{C}_{21}\text{H}_{21}\text{NZr}$  (378.62): C, 66.62; H, 5.59; N, 3.70. Found: C, 65.91; H, 6.10; N, 3.29.  $^1\text{H}$  NMR (400 MHz, benzene- $d_6$ ):  $\delta$  6.71 (t, 1H,  $\text{C}_6\text{H}_3$ ), 6.56 (d, 2H,  $\text{C}_6\text{H}_3$ ), 5.46 (s, 5H,  $\text{C}_5\text{H}_5$ ), 4.89 (s, 7H,  $\text{C}_7\text{H}_7$ ), 2.03 (s, 6H,  $\text{CCH}_3$ ).  $^{13}\text{C}$  NMR (100.53 MHz, benzene- $d_6$ ):  $\delta$  171.3 (CNR), 134.9 (*i*- $\text{C}_6\text{H}_3$ ), 128.8 ( $\text{C}_6\text{H}_3$ ), 128.1 ( $\text{C}_6\text{H}_3$ ), 127.8 ( $\text{C}_6\text{H}_3$ ), 98.4 ( $\text{C}_5\text{H}_5$ ), 82.0 ( $\text{C}_7\text{H}_7$ ), 18.6 ( $\text{CCH}_3$ ). IR (KBr):  $\nu$  2134  $\text{cm}^{-1}$  ( $\text{C}\equiv\text{N}$ ). We assume that the elemental analyses are not perfectly satisfactory due to partial loss of the isocyanide ligand.

**Single-Crystal X-ray Structure Determination of Compounds 1 and 2a.** Crystal data and details of the structure determination are presented in Table 4. Suitable single crystals of **1** (**2a**) for the X-ray diffraction study were grown from THF. A clear purple fragment (orange fragment) was stored under perfluorinated ether, transferred to a Lindemann capillary, fixed, and sealed. Preliminary examination and data collection were carried out on an area detecting system (NONIUS, MACH3,  $\kappa$ -CCD) at the window of a rotating anode (NONIUS, FR951) with graphite-monochromated  $\text{Mo K}\alpha$  radiation ( $\lambda = 0.71073 \text{ \AA}$ ). The unit cell parameters were obtained by full-matrix least-squares refinement of 1059 (1694) reflections. Data collection were performed at 133 (133) K (OXFORD CRYOSYSTEMS) within a  $\theta$  range of  $3.08^\circ < \theta < 25.39^\circ$  ( $2.19^\circ < \theta < 25.37^\circ$ ). Each compound was measured with nine data sets in the rotation scan mode with  $\Delta\varphi/\Delta\omega = 2.0^\circ$  ( $1.0^\circ$ ). A total number of 23 575 (35 406) intensities were

(50) Hitchcock, P. B.; Lappert, M. F.; Liu, D.; Ryan, E. J. *Polyhedron* **1995**, *14*, 2745.

(51) (a) Data Collection Software for Nonius  $\kappa$ -CCD devices, Delft, The Netherlands, 2001. (b) Otwinowski, Z.; Minor, W. *Methods Enzymol.* **1997**, *276*, 307. (c) Altomare, A.; Cascarano, G.; Giacovazzo, C.; Guagliardi, A.; Burla, M. C.; Polidori, G.; Camalli, M. SIR92. *J. Appl. Crystallogr.* **1994**, *27*, 435–436. (d) *International Tables for Crystallography*; Wilson, A. J. C., Ed.; Kluwer Academic: Dordrecht, The Netherlands, 1992; Vol. C, Tables 6.1.1.4, 4.2.6.8, and 4.2.4.2. (e) Spek, A. L. PLATON, A Multipurpose Crystallographic Tool; Utrecht University, Utrecht, The Netherlands, 2001. (f) Sheldrick, G. M., SHELXL-97; Universität Göttingen, Göttingen, Germany, 1998.

(52) Li, J.; Bursten, B. E. *J. Am. Chem. Soc.* **1997**, *119*, 9021.



Table 4. Crystallographic Data for **1** and **2a**

	<b>1</b>	<b>2a</b>
formula	C <sub>12</sub> H <sub>12</sub> Zr	C <sub>17</sub> H <sub>21</sub> NZr
fw	247.44	330.57
color/habit	purple/fragment	orange/fragment
cryst dimens (mm <sup>3</sup> )	0.08 × 0.20 × 0.36	0.20 × 0.38 × 0.56
cryst syst	orthorhombic	orthorhombic
space group	<i>Pnma</i> (No. 62)	<i>Pbcm</i> (No. 57)
<i>a</i> , Å	11.1033(2)	8.3304(1)
<i>b</i> , Å	10.5715(2)	18.5959(2)
<i>c</i> , Å	8.2212(1)	10.1241(1)
<i>V</i> , Å <sup>3</sup>	964.99(3)	1568.34(3)
<i>Z</i>	4	4
<i>T</i> , K	133	133
<i>D</i> <sub>calcd</sub> , g cm <sup>-3</sup>	1.703	1.400
<i>μ</i> , mm <sup>-1</sup>	1.084	0.688
<i>F</i> (000)	496	680
<i>θ</i> range, deg	3.08–25.39	2.19–25.37
index ranges ( <i>hkl</i> )	±13, ±12, ±9	±10, ±22, ±12
no. of rflns collected	23575	35406
no. of indep rflns/ <i>R</i> <sub>int</sub>	935/0.036	1532/0.035
no. of obsd rflns ( <i>I</i> > 2σ( <i>I</i> ))	897	1456
no. of data/restraints/ params	935/0/90	1532/0/98
<i>R</i> <sub>1</sub> / <i>wR</i> <sub>2</sub> ( <i>I</i> > 2σ( <i>I</i> )) <sup>a</sup>	0.0143/0.0334	0.0242/0.0571
<i>R</i> <sub>1</sub> / <i>wR</i> <sub>2</sub> (all data) <sup>a</sup>	0.0155/0.0338	0.0255/0.0580
GOF (on <i>F</i> <sup>2</sup> ) <sup>a</sup>	1.101	1.089
largest diff peak and hole (e Å <sup>-3</sup> )	+0.28 / -0.22	+0.52 / -0.43

<sup>a</sup> *R*<sub>1</sub> = Σ(|*F*<sub>o</sub>| - |*F*<sub>c</sub>|)/Σ|*F*<sub>o</sub>|; *wR*<sub>2</sub> = {Σ[*w*(*F*<sub>o</sub><sup>2</sup> - *F*<sub>c</sub><sup>2</sup>)]/Σ[*w*(*F*<sub>o</sub><sup>2</sup>)]}<sup>1/2</sup>;  
GOF = {Σ[*w*(*F*<sub>o</sub><sup>2</sup> - *F*<sub>c</sub><sup>2</sup>)]/(*n* - *p*)<sup>1/2</sup>.

integrated. Raw data were corrected for Lorentz and polarization effects and, arising from the scaling procedure, for latent decay and absorption effects. After merging (*R*<sub>int</sub> = 0.036 (0.035)) a sum of 935 (1532) (all data) and 897 (1456) data (*I* > 2σ(*I*)), respectively, remained, and all data were used. The structures were solved by a combination of direct methods and difference Fourier syntheses. All non-hydrogen atoms were refined with anisotropic displacement parameters. **1**: all

hydrogen atoms were found and refined with individual isotropic displacement parameters. **2a**: all hydrogen atoms were placed in ideal positions (riding model). Full-matrix least-squares refinements with 90 (98) parameters were carried out by minimizing Σ*w*(*F*<sub>o</sub><sup>2</sup> - *F*<sub>c</sub><sup>2</sup>)<sup>2</sup> with the SHELXL-97 weighting scheme and stopped at a shift to error ratio of <0.001 (0.001). The final residual electron density maps showed no remarkable features. Neutral atom scattering factors for all atoms and anomalous dispersion corrections for the non-hydrogen atoms were taken from the International Tables for Crystallography. All calculations were performed on an Intel Pentium II PC, with the STRUX-V system, including the programs PLATON, SIR92, and SHELXL-97.<sup>51</sup> **1** and **2a**: both compounds are located on a crystallographic mirror plane. Crystallographic data (excluding structure factors) for the structures reported in this paper have been deposited with the Cambridge Crystallographic Data Centre as Supplementary Publication Nos. CCDC-265527 (**1**) and CCDC-265526 (**2a**). Copies of the data can be obtained free of charge on application to the CCDC, 12 Union Road, Cambridge CB2 1EZ, U.K. (fax, (+44)1223-336-033; e-mail, deposit@ccdc.cam.ac.uk).

**Acknowledgment.** This work was financially supported by the Deutsche Forschungsgemeinschaft. We wish to thank Dr. K. Ruhland for helpful discussions. M.T. is grateful to Prof. W. A. Herrmann (Munich) for the appointment to temporarily represent the Chair of Inorganic Chemistry at the Technische Universität München.

**Supporting Information Available:** Details of the electronic structure calculations, presentations of the calculated molecular structures of **1**, **2a**, and **2b** as well as of the isocyanides *t*BuNC and *o*-XyNC together with Cartesian coordinates of their atomic positions, and crystallographic data in the CIF format. This material is available free of charge via the Internet at <http://pubs.acs.org>.

OM050192C